Strongly magnetized neutron star matter in the extended Zimanyi-Moszkowski model

K Miyazaki

E-mail: miyazakiro@rio.odn.ne.jp

Abstract. We investigate the neutron star matter in magnetic field using the extended Zimanyi-Moszkowski model. The anomalous magnetic moments of nucleons and the isovector-scalar mean-field are taken into account. We calculate the renormalized nucleon masses and the equations-of-state as functions of the total baryon density for several strengths of magnetic field. It is found that only the ultra strong field $B > 10^{19}G$ is effective in the results. We further investigate the dependencies of the renormalized masses and the particle fractions upon the magnetic field. In weak field $B < 10^{16}G$ they are constant, while the effects of Landau quantization are apparent as the field becomes stronger. Although almost the features of our results are essentially the same as those in the preceding works, we cannot reproduce the anomalous features in $B = 10^{13}G$ predicted by F.X. Wei *et al* .

1. Introduction

It has been well known that the neutron stars (NSs) observed as radio pulsars have strong magnetic fields $B = 10^{12} \sim 10^{13}G$ on their surfaces. Although these strengths are already by far stronger than the magnetic fields achieved in laboratories and detected on the other stars, there are the other classes of NSs observed as the soft gamma repeaters and the anomalous x-ray pulsars that have much stronger magnetic fields $B = 10^{14} \sim 10^{15}G$. They are called as the magnetars [1-3] and there have been found their candidates more than 10 so far.

The magnetic fields of magnetars are stronger than the critical value $B_C(e) = m_e/(2\mu_B) = 4.414 \times 10^{13}G$ for electrons. The surface structure of magnetar is therefore quite different from the ordinary NS [4]. On the contrary, the cores of magnetars and NSs are the hadronic matters composed of nucleons, hyperons and condensed mesons along with leptons. Because the critical value $B_C(N) = M_N/(2\mu_N) = 1.488 \times 10^{20}G$ for nucleons is extremely strong, even the magnetic fields $B = 10^{14} \sim 10^{15}G$ cannot affect the properties of the cores of magnetars.

However, according to the expectation that the magnetic field in the core of magnetar becomes much stronger than its surface, the strongly magnetized NS matter was first investigated in Ref. [5]. This work used the relativistic mean-field (RMF) theory [6-8] of nuclear matter because it is more appropriate to dense baryonic matter than the nonrelativistic theories. Moreover, it is worthwhile to note that within the

RMF models the mass of nucleon in dense medium is largely reduced from its free value, and so the critical field for nucleons in NSs might become weaker than $1.488 \times 10^{20}G$. Because of these reasons all the subsequent works to Ref. [5] rely on the RMF models.

Although Ref. [5] investigated NS matter within the original Walecka σ-ω model [6], the later work [9] employed the nonlinear Walecka (NLW) and the Zimanyi-Moszkowski (ZM) [10] models. The NLW model is the most widely used in the investigations of nuclear physics. However, the meson self-coupling terms have parameters that are adjusted to reproduce the properties of finite nuclei, and so we cannot believe that the model is really valid at higher densities than nuclear matter saturation. In this respect, the RMF models, which have explicit or implicit density dependence, are desirable. The ZM model is such a model being applicable to the magnetized NS matter. It has a renormalized $NN\sigma$ coupling constant by the renormalized nucleon mass M_N^*/M_N. However, its $NN\omega$ coupling constant is not renormalized, and the renormalized mass $M_N^* = 0.85M_N$ is too large to reproduce the spin-orbit splitting of finite nuclei.

The above two works did not take into account the anomalous magnetic moments (AMMs) of nucleons nor the effect of muons. They were first considered in Ref. [11]. The latest work [12] further takes into account the isovector-scalar δ-meson. It predicts that the equation-of-state (EOS) becomes stiffer for $B = 10^{12} \sim 10^{13}G$ than $B = 0$ and $B > 10^{15}G$. If the result is true, the structures of the ordinary NSs observed as radio pulsars are largely altered from the previous investigations without the magnetic field.

In the present work, we reinvestigate the strongly magnetized NS matter within the extended Zimanyi-Moszkowski (EZM) model [13,14]. The model is the modification and extension of the original ZM model based on the consistent quark picture of nucleons (or baryons). It can overcome the above-mentioned shortcomings of the NLW and ZM models. Especially, the EZM model predicts the same saturation properties of nuclear matter [13] as the Dirac-Brueckner-Hartree-Fock (DBHF) theory [15] and reproduces the empirical critical temperature of liquid-gas phase transition in nuclear matter [16]. It has been further applied [17-26] to various subjects of nuclear physics and astrophysics. In some aspects the EZM model reproduces the similar properties to the NLW model, while in other aspects it shows essentially different features. It is therefore worthwhile to apply the EZM model to the NS matter in strong magnetic fields. Our main purpose is to compare the EZM model with the NLW and the original ZM models and to investigate the effect of δ-meson. In the next section we develop the formulation of the EZM model. In section 3 the numerical results are shown and discussed. Finally, the present work is summarized in section 4.

2. The EZM model

Here we reformulate the EZM model of NS matter in the magnetic field B. In the present work we consider only nucleons as baryons so as to compare the preceding works [11,12].

The model Lagrangian of the NS matter in the mean-field approximation is

$$\begin{aligned}\mathcal{L} = & \sum_{N=p,\,n} \bar{\psi}_N \left(\not{p} - q_N \not{A} - \frac{1}{2}\,\kappa_N \sigma_{\mu\nu} F^{\mu\nu} - M_N^* - \gamma^0 V_N \right) \psi_N \\ & + \sum_{l=e^-,\,\mu^-} \bar{\psi}_l \left(\not{p} + e\,\not{A} - m_l \right) \psi_l \\ & - \frac{1}{2}\, m_\sigma^2 \langle\sigma\rangle^2 - \frac{1}{2}\, m_\delta^2 \langle\delta_3\rangle^2 + \frac{1}{2}\, m_\omega^2 \langle\omega_0\rangle^2 + \frac{1}{2}\, m_\rho^2 \langle\rho_{03}\rangle^2 \,, \end{aligned} \tag{1}$$

where ψ_N and ψ_l are the Dirac fields of nucleons and leptons. The charges of nucleons are $q_p = e\,(>0)$ and $q_n = 0$ and κ_N is their AMM. The electromagnetic vector potential $A^\mu = (0, 0, xB, 0)$ is for the external magnetic filed B along the z-axis and $F^{\mu\nu} = \partial^\mu A^\nu - \partial^\nu A^\mu$. The isoscalar-scalar, isoscalar-vector, isovector-scalar and isovector-vector mean-fields are $\langle\sigma\rangle$, $\langle\omega_0\rangle$, $\langle\delta_3\rangle$ and $\langle\rho_{03}\rangle$, respectively. The mass of each meson is m_σ, m_ω, m_δ and m_ρ. The renormalized mass of nucleons M_N^* in the matter is defined by

$$M_N^* = M_N + S_N, \tag{2}$$

where the scalar potential S_N is

$$S_p = -g_{pp\sigma}^* \langle\sigma\rangle - g_{pp\,\delta}^* \langle\delta_3\rangle \,, \tag{3}$$

$$S_n = -g_{nn\sigma}^* \langle\sigma\rangle + g_{nn\delta}^* \langle\delta_3\rangle \,. \tag{4}$$

The vector potential V_N in Eq. (1) is

$$V_p = g_{pp\,\omega}^* \langle\omega_0\rangle + g_{pp\rho}^* \langle\rho_{03}\rangle \,, \tag{5}$$

$$V_n = g_{nn\omega}^* \langle\omega_0\rangle - g_{nn\rho}^* \langle\rho_{03}\rangle \,. \tag{6}$$

The renormalized coupling constants in Eqs. (3)-(5) are given [13,14] by

$$g_{pp\,\sigma(\omega)}^* \equiv h_{pp\sigma(\omega)}^* g_{NN\sigma(\omega)} = \left[(1-\lambda) + \lambda m_p^* \right] g_{NN\sigma(\omega)}, \tag{7}$$

$$g_{nn\sigma(\omega)}^* \equiv h_{nn\sigma(\omega)}^* g_{NN\sigma(\omega)} = \left[(1-\lambda) + \lambda m_n^* \right] g_{NN\sigma(\omega)}, \tag{8}$$

$$g_{pp\delta(\rho)}^* \equiv h_{pp\delta(\rho)}^* g_{NN\delta(\rho)} = \left[(1-\lambda) + \lambda \left(2m_n^* - m_p^* \right) \right] g_{NN\delta(\rho)}, \tag{9}$$

$$g_{nn\delta(\rho)}^* \equiv h_{nn\delta(\rho)}^* g_{NN\delta(\rho)} = \left[(1-\lambda) + \lambda \left(2m_p^* - m_n^* \right) \right] g_{NN\delta(\rho)}, \tag{10}$$

where $g_{NN\sigma(\omega,\,\delta,\,\rho)}$ is the free coupling constant and $\lambda = 1/3$.

The total energy density of matter is given by

$$\mathcal{E} = \sum_{i=p,\,n,\,e^-,\,\mu^-} \varepsilon_i + \sum_{N=p,\,n} V_N \rho_N + \frac{1}{2}\, m_\sigma^2 \langle\sigma\rangle^2 + \frac{1}{2}\, m_\delta^2 \langle\delta_3\rangle^2 - \frac{1}{2}\, m_\omega^2 \langle\omega_0\rangle^2 - \frac{1}{2}\, m_\rho^2 \langle\rho_{03}\rangle^2 \,. \tag{11}$$

The energy density of each particle is [5,9,11]

$$\varepsilon_p = \frac{\mu_N M_N B}{2\pi^2} \sum_{s=-1,1} \sum_{\nu}^{\nu_p^{\max}} \left\{ E_{Fp} k_{Fp}(\nu,s) + \bar{M}_p(\nu,s)^2 \ln \left| \frac{E_{Fp} + k_{Fp}(\nu,s)}{\bar{M}_p(\nu,s)} \right| \right\}, \tag{12}$$

$$\begin{aligned} \varepsilon_n = \frac{1}{4\pi^2} \sum_{s=-1,1} \Bigg\{ & \frac{1}{2} E_{Fn}^3 k_{Fn}(s) + \frac{2}{3} s\,\kappa_n B E_{Fn}^3 \left[\arcsin \frac{\bar{M}_n(s)}{E_{Fn}} - \frac{\pi}{2} \right] \\ & + \left[\frac{1}{3} s\,\kappa_n B - \frac{1}{4} \bar{M}_n(s) \right] \left[\bar{M}_n(s) k_{Fn}(s) E_{Fn} + \bar{M}_n(s)^3 \ln \left| \frac{E_{Fn} + k_{Fn}(s)}{\bar{M}_n(s)} \right| \right] \Bigg\}, \end{aligned} \tag{13}$$

$$\varepsilon_e = \frac{\mu_B m_e B}{2\pi^2} \sum_{\nu=0}^{\nu_e^{\max}} g(\nu) \left\{ E_{Fe} k_{Fe}(\nu) + \bar{m}_e(\nu)^2 \ln \left| \frac{E_{Fe} + k_{Fe}(\nu)}{\bar{m}_e(\nu)} \right| \right\}, \tag{14}$$

$$\varepsilon_\mu = \frac{\mu_\mu m_\mu B}{2\pi^2} \sum_{\nu=0}^{\nu_\mu^{\max}} g(\nu) \left\{ E_{F\mu} k_{F\mu}(\nu) + \bar{m}_\mu(\nu)^2 \ln \left| \frac{E_{F\mu} + k_{F\mu}(\nu)}{\bar{m}_\mu(\nu)} \right| \right\}, \tag{15}$$

where μ_N, μ_B and μ_μ are nuclear magneton, Bohr magneton and muon magneton, respectively. The Landau quantum number ν in Eq. (12) starts from 0 for spin-down ($s = -1$) and 1 for spin-up ($s = 1$). The spin degenerate factor $g(\nu)$ in Eqs. (14) and (15) is 1 for $\nu = 0$ but 2 for $\nu \geq 1$. The effective mass of each particle on each Landau level is defined as

$$\bar{M}_p(\nu,s) = \left(M_p^{*2} + 4\,\nu\,\mu_N M_N B \right)^{1/2} + s\,\kappa_p B, \tag{16}$$

$$\bar{M}_n(s) = M_n^* + s\,\kappa_n B, \tag{17}$$

$$\bar{m}_e(\nu) = \left(m_e^2 + 4\,\nu\,\mu_B m_e B \right)^{1/2}, \tag{18}$$

$$\bar{m}_\mu(\nu) = \left(m_\mu^2 + 4\,\nu\,\mu_\mu m_\mu B \right)^{1/2}. \tag{19}$$

The Fermi energies are determined from the chemical potentials

$$E_{Fp(n)} = \mu_{p(n)} - V_{p(n)}, \tag{20}$$

$$E_{Fe(\mu)} = \mu_{e(\mu)}. \tag{21}$$

In NS matter the β-equilibrium condition

$$\mu_n - \mu_p = \mu_e = \mu_\mu \tag{22}$$

is satisfied. (Do not confuse the magnetons with the chemical potentials.) The Fermi momentum of each particle on each Landau level is given by

$$k_{Fp}(\nu,s) = \left[E_{Fp}^2 - \bar{M}_p(\nu,s)^2 \right]^{1/2}, \tag{23}$$

$$k_{Fn}(s) = \left[E_{Fn}^2 - \bar{M}_n(s)^2 \right]^{1/2}, \tag{24}$$

$$k_{Fe(\mu)}(\nu) = \left[E_{Fe(\mu)}^2 - \bar{m}_{e(\mu)}(\nu)^2 \right]^{1/2}. \tag{25}$$

The condition that the Fermi momenta are real values restricts the maximum value of the quantum number ν for each particle. The baryon density ρ_N in the second term of Eq. (11) is defined as [11,12]

$$\rho_p = \frac{\mu_N M_N B}{\pi^2} \sum_{s=-1,1} \sum_{\nu}^{\nu_p^{\max}} k_{Fp}(\nu, s), \tag{26}$$

$$\rho_n = \frac{1}{2\pi^2} \sum_{s=-1,1} \left\{ \frac{1}{3} k_{Fn}(s)^3 + \frac{1}{2} s \kappa_n B \left[\bar{M}_n(s) k_{Fn}(s) + E_{Fn}^2 \left(\arcsin \frac{\bar{M}_n(s)}{E_{Fn}} - \frac{\pi}{2} \right) \right] \right\}. \tag{27}$$

Similarly, the lepton densities are [5,9]

$$\rho_e = \frac{\mu_B m_e B}{\pi^2} \sum_{\nu=0}^{\nu_e^{\max}} g(\nu) k_{Fe}(\nu), \tag{28}$$

$$\rho_\mu = \frac{\mu_\mu m_\mu B}{\pi^2} \sum_{\nu=0}^{\nu_\mu^{\max}} g(\nu) k_{F\mu}(\nu). \tag{29}$$

From Eqs. (2)-(4) the scalar meson mean-fields $\langle\sigma\rangle$ and $\langle\delta_3\rangle$ are expressed by the renormalized masses M_p^* and M_n^*. From Eqs. (5) and (6) the vector meson mean-fields $\langle\omega_0\rangle$ and $\langle\rho_{03}\rangle$ are expressed by the vector potentials V_p and V_n. The total energy density $\mathcal{E}$ of Eq. (11) is therefore expressed by M_N^* and V_N. Then, they are determined by extremizing the energy, $\partial\mathcal{E}/\partial M_N^* = 0$ and $\partial\mathcal{E}/\partial V_N = 0$. Consequently, we have the self-consistency equations:

$$\begin{aligned} \frac{\rho_p}{M_N} \left(C^{(0)}\right)^2 &- \left[\left(\frac{m_\omega}{g_{NN\omega}} \right)^2 \left(h_{nn\rho}^*\right)^2 + \left(\frac{m_\rho}{g_{NN\rho}} \right)^2 (h_{nn\omega}^*)^2 \right] v_p \\ &- \left[\left(\frac{m_\omega}{g_{NN\omega}} \right)^2 h_{pp\rho}^* h_{nn\rho}^* - \left(\frac{m_\rho}{g_{NN\rho}} \right)^2 h_{pp\omega}^* h_{nn\omega}^* \right] v_n = 0, \end{aligned} \tag{30}$$

$$\begin{aligned} \frac{\rho_n}{M_N} \left(C^{(0)}\right)^2 &- \left[\left(\frac{m_\omega}{g_{NN\omega}} \right)^2 h_{pp\rho}^* h_{nn\rho}^* - \left(\frac{m_\rho}{g_{NN\rho}} \right)^2 h_{pp\omega}^* h_{nn\omega}^* \right] v_p \\ &- \left[\left(\frac{m_\omega}{g_{NN\omega}} \right)^2 \left(h_{pp\rho}^*\right)^2 + \left(\frac{m_\rho}{g_{NN\rho}} \right)^2 \left(h_{pp\omega}^*\right)^2 \right] v_n = 0, \end{aligned} \tag{31}$$

$$\begin{aligned} &\frac{\rho_p^{(S)}}{M_N} \left(C^{(0)}\right)^3 + \left(\frac{m_\sigma}{g_{NN\sigma}} \right)^2 A^{(0)} \left(A_p^{(1)} C^{(0)} - A^{(0)} C_p^{(1)} \right) + \left(\frac{m_\delta}{g_{NN\delta}} \right)^2 B^{(0)} \left(C^{(0)} - B^{(0)} C_p^{(1)} \right) \\ &- \lambda \left(\frac{m_\omega}{g_{NN\omega}} \right)^2 \left(h_{nn\rho}^* v_p + h_{pp\rho}^* v_n \right) \left\{ \left[\left(h_{pp\rho}^*\right)^2 - \left(h_{nn\rho}^*\right)^2 + h_{pp\omega}^* h_{pp\rho}^* + h_{nn\omega}^* h_{nn\rho}^* \right] v_p \right. \\ &\qquad \left. - \left[\left(h_{pp\omega}^* + h_{pp\rho}^* \right) h_{nn\rho}^* + \left(h_{nn\omega}^* + h_{nn\rho}^* \right) h_{pp\rho}^* \right] v_n \right\} \\ &+ \lambda \left(\frac{m_\rho}{g_{NN\rho}} \right)^2 \left(h_{nn\omega}^* v_p - h_{pp\omega}^* v_n \right) \left[2 h_{nn\omega}^* h_{nn\rho}^* v_p + \left(h_{nn\omega}^* h_{pp\rho}^* - h_{pp\omega}^* h_{nn\rho}^* \right) v_n \right] = 0, \end{aligned} \tag{32}$$

$$\frac{\rho_n^{(S)}}{M_N}\left(C^{(0)}\right)^3+\left(\frac{m_\sigma}{g_{NN\sigma}}\right)^2 A^{(0)}\left(A_n^{(1)}C^{(0)}-A^{(0)}C_n^{(1)}\right)-\left(\frac{m_\delta}{g_{NN\delta}}\right)^2 B^{(0)}\left(C^{(0)}+B^{(0)}C_n^{(1)}\right)$$
$$-\lambda\left(\frac{m_\omega}{g_{NN\omega}}\right)^2\left(h^*_{nn\rho}v_p+h^*_{pp\rho}v_n\right)\left\{\left[\left(h^*_{nn\rho}\right)^2-\left(h^*_{pp\rho}\right)^2+h^*_{pp\omega}h^*_{pp\rho}+h^*_{nn\omega}h^*_{nn\rho}\right]v_n\right.$$
$$\left.-\left[\left(h^*_{pp\omega}+h^*_{pp\rho}\right)h^*_{nn\rho}+\left(h^*_{nn\omega}+h^*_{nn\rho}\right)h^*_{pp\rho}\right]v_p\right\}$$
$$-\lambda\left(\frac{m_\rho}{g_{NN\rho}}\right)^2\left(h^*_{nn\omega}v_p-h^*_{pp\omega}v_n\right)\left[2h^*_{pp\omega}h^*_{pp\rho}v_n+\left(h^*_{pp\omega}h^*_{nn\rho}-h^*_{pp\rho}h^*_{nn\omega}\right)v_p\right]=0, \quad (33)$$

where we have introduced $V_{p(n)}=v_{p(n)}M_N$ and

$$A^{(0)}=h^*_{nn\delta}\left(m^*_p-1\right)+h^*_{pp\delta}\left(m^*_n-1\right), \quad (34)$$

$$B^{(0)}=h^*_{nn\sigma}\left(m^*_p-1\right)-h^*_{pp\sigma}\left(m^*_n-1\right), \quad (35)$$

$$C^{(0)}=h^*_{pp\sigma}h^*_{nn\delta}+h^*_{nn\sigma}h^*_{pp\delta}=h^*_{pp\omega}h^*_{nn\rho}+h^*_{nn\omega}h^*_{pp\rho}, \quad (36)$$

$$A_p^{(1)}=(1-2\lambda)+2\lambda\left(2m^*_p-m^*_n\right), \quad (37)$$

$$C_p^{(1)}=2\lambda\, h^*_{nn\delta}, \quad (38)$$

$$A_n^{(1)}=(1-2\lambda)+2\lambda\left(2m^*_n-m^*_p\right), \quad (39)$$

$$C_n^{(1)}=2\lambda\, h^*_{pp\delta}. \quad (40)$$

The scalar densities of the first terms in Eqs. (32) and (33) are [11,12]

$$\rho_p^{(S)}=\frac{\mu_N M_p^* M_N B}{\pi^2}\sum_{s=-1,1}\sum_{\nu}^{\nu_p^{\max}}\frac{\bar{M}_p(\nu,s)}{\bar{M}_p(\nu,s)-s\,\kappa_p B}\ln\left|\frac{E_{Fp}+k_{Fp}(\nu,s)}{\bar{M}_p(\nu,s)}\right|, \quad (41)$$

$$\rho_n^{(S)}=\frac{M_n^*}{4\pi^2}\sum_{s=-1,1}\left\{E_{Fn}k_{Fn}(s)-\bar{M}_n(s)^2\ln\left|\frac{E_{Fn}+k_{Fn}(s)}{\bar{M}_n(s)}\right|\right\}. \quad (42)$$

The baryon and scalar densities are determined from the chemical potentials. Due to Eq. (22) there are only two independent chemical potentials, which are constrained by the baryon number conservation

$$\rho_B=\rho_p+\rho_n, \quad (43)$$

and the charge neutral condition

$$\rho_p=\rho_e+\rho_\mu. \quad (44)$$

3. Numerical analyses

For calculating in RMF model, we have to specify the meson-nucleon coupling constants. The $NN\sigma$ and $NN\omega$ coupling constants $(g_{NN\sigma}/m_\sigma)^2 = 16.9\,\mathrm{fm}^2$ and $(g_{NN\omega}/m_\omega)^2 = 12.5\,\mathrm{fm}^2$ have been determined in Ref. [13] so as to reproduce the nuclear matter saturation properties. On the other hand, the $NN\delta$ coupling constant $(g_{NN\delta}/m_\delta)^2 = 2.5\,\mathrm{fm}^2$ is assumed to be the same as Ref. [12] because our results are compared with those in the work. Then, the $NN\rho$ coupling constant $(g_{NN\rho}/m_\rho)^2 = 3.005\,\mathrm{fm}^2$ is determined so as to reproduce the empirical symmetry energy of nuclear matter $E_s = 32.0\mathrm{MeV}$ [27]. It is however noted that both the $NN\delta$ and $NN\rho$ coupling constants are much stronger than the physically reasonable values $(g_{NN\delta}/m_\delta)^2 = 0.39\,\mathrm{fm}^2$ and $(g_{NN\rho}/m_\rho)^2 = 0.82\,\mathrm{fm}^2$ in the Bonn A potential [15]. Therefore, the results in the present work will magnify the effect of isovector contributions.

Once determining the coupling constants, for a definite density ρ_B in Eq. (43) we can solve the selfconsistent equations (30)-(33), (43) and (44) in terms of 6-dimensional Newton-Raphson method so that the renormalized masses M_p^* and M_n^*, the vector potentials V_p and V_n, and the chemical potentials μ_p and μ_n are calculated. Figure 1 shows the renormalized masses $m_N^* \equiv M_N^*/M_N$ as functions of ρ_B. We first calculate for no magnetic field $B = 0$. Secondly, $B = 10^{13}G$ is the field for which the anomalous features have been observed in Ref. [12]. Next, $B = 10^5 B_C(e)$ is approximate to the maximum interior field of NSs [28] expected from the scalar virial theorem. Finally, the ultra strong field $B = 10^6 B_C(e)$ is chosen as an extreme limit. The black and red curves are the results of proton and neutron. The upper and lower panels are the results without and with the AMMs. The differences between m_p^* and m_n^* are due to the isovector-scalar mean-field $\langle\delta_3\rangle$. For $B = 0$, because of the strong $NN\delta$ coupling constant, m_n^* becomes negative above $\rho_B = 1.2\,\mathrm{fm}^{-3}$ at which we have stopped our calculations. This is not a problem because the RMF theories of point-like nucleons lose their meanings at such high densities and because the central baryon densities of NSs are lower than $\rho_B = 1.2\,\mathrm{fm}^{-3}$. On the other hand, in Refs. [11] and [12] the renormalized masses are positive even at much higher densities. This is mainly because their renormalized masses of nucleon at saturation are much larger than our result $m_N^* = 0.603$. It has been however known [29,30] that $m_N^* \simeq 0.6$ is reasonable to reproduce the spin-orbit splitting of finite nuclei. Moreover, their $NN\omega$ coupling constants are much weaker than ours, although our value is close to the physically reasonable coupling of the Bonn A potential [15].

First, we see in the upper panel that the external magnetic field cannot affect the renormalized masses except for the ultra strong field $B = 10^6 B_C(e)$ in which m_p^* is suppressed obviously but m_n^* is enhanced slightly, and so m_n^* is always larger than m_p^*. Even if the AMMs are taken into account (in the lower panel), the magnetic field is also effective only for $B = 10^6 B_C(e)$ in which m_n^* is enhanced obviously while m_p^* is suppressed below but is enhanced above $\rho_B = 0.48\,\mathrm{fm}^{-3}$. As a result m_n^* is larger than m_p^* below $\rho_B = 0.6\,\mathrm{fm}^{-3}$. Although these features have been also found in Ref. [12], we cannot reproduce the large enhancement of m_p^* for $B = 10^{13}G$ predicted in Ref. [12].

Figure 2 shows the EOSs of NS matter for the same magnetic fields as Fig. 1. The pressure is calculated in terms of the Gibbs-Duhem relation $P = \mu_n \rho_B - \mathcal{E}$. We also see that only the ultra strong magnetic field affects the EOS. This is the natural result of Fig. 1. Without the AMMs, the EOS for $B = 10^6 B_C(e)$ becomes softer at lower densities while becomes stiffer at higher densities. Below $\rho_B = 0.2\,\mathrm{fm}^{-3}$ the pressure becomes negative according to the fact that the NS matter in such a strong magnetic field becomes self-bound as has been already found in Refs. [5] and [9]. Taking into account the AMMs, the EOS becomes much stiffer although the pressure is also negative below $\rho_B = 0.12\,\mathrm{fm}^{-3}$. Again, we cannot find the stiff EOSs for $B = 10^{13}G$ predicted in Ref. [12].

In order to investigate the dependencies on the magnetic field in detail, Fig. 3 shows the renormalized masses as functions of $B/B_C(e)$ for $\rho_B = 0.08$, 0.16, 0.32 and $0.64\mathrm{fm}^{-3}$. The black and red curves are for proton and neutron, respectively. Without the AMMs (the upper panel), the masses are almost constant below $B = 10^5 B_C(e)$, while above the strength m_p^* turns to decrease but m_n^* is slightly enhanced, and so m_n^* becomes larger than m_p^* in the ultra strong field. Taking into account the AMMs (the lower panel), the similar features are found for lower densities $\rho_B \leq 0.32\,\mathrm{fm}^{-3}$ while for high density $\rho_B = 0.64\,\mathrm{fm}^{-3}$ both m_p^* and m_n^* turn to increase above $B = 5.0 \times 10^{15} B_C(e)$.

Figure 4 shows the proton (the black curves) and muon (the red curves) fractions as functions of $B/B_C(e)$ for the same densities as Fig. 3 without (the upper panel) and with (the lower panel) the AMMs. In weaker magnetic fields the fractions are almost constant. As the field becomes stronger, the fractions begin to oscillate and the oscillations become more intense. These phenomena are the signals of the Landau quantization because the maximum quantum number $\nu_p^{\max}$ decreases and the intervals between the Landau levels widen. As the field becomes much stronger, the proton is completely polarized and so its fraction turns to increase monotonically. In the ultra strong field the protons are more abundant than neutrons. To the contrary, the muons disappear above $B = 10^5 B_C(e)$ because the Fermi energy of muon is the same as electron but the muon mass is much heavier than the electron mass.

In the weak magnetic fields $B \ll B_C(N)$, the effects of AMMs are neglected. In this case, no physical quantities of neutron depend on the magnetic field. On the other hand, any physical quantity of proton is generally expressed by

$$\langle Q \rangle = \frac{\mu_N M_N B}{\pi^2} \sum_{\nu=0}^{\nu_p^{\max}} g(\nu) \int_0^{k_{Fp}(\nu)} dk\, Q(k,\nu), \tag{45}$$

where $Q(k,\nu) = 1$ for the baryon density ρ_p, $Q(k,\nu) = \left(k^2 + \bar{M}_p(\nu)^2\right)^{1/2}$ for the energy density ε_p and $Q(k,\nu) = \partial\left(k^2 + \bar{M}_p(\nu)^2\right)^{1/2}/\partial M_p^*$ for the scalar density. Then, we can approximate the summation of the Landau quantum number ν by the integral of

$\xi = 2\nu\mu_N B/M_N$, (see Eq. (16))

$$\langle Q\rangle \simeq \frac{M_N^2}{\pi^2}\int_0^{k_{Fp}^2/(2M_N^2)} d\xi \int_0^{k_{Fp}(\xi)} dk\, Q(k,\xi), \tag{46}$$

where $k_{Fp}^2 = E_{Fp}^2 - M_p^{*2}$. The upper limit of ξ is determined from $k_{Fp}(\xi)^2 = k_{Fp}^2 - 2\,\xi M_N^2 = 0$ due to the same reason as restricting $\nu_p^{\max}$ mentioned below Eq. (25). Consequently, $\langle Q\rangle$ does not depend on the magnetic field B. This indicates that in $B \ll B_C(N)$ we have the same results as $B = 0$. In fact, the baryon density is

$$\rho_p \simeq \frac{M_N^2}{\pi^2}\int_0^{k_{Fp}^2/(2M_N^2)} d\xi \left(k_{Fp}^2 - 2\,\xi M_N^2\right)^{1/2} = \frac{1}{2\pi^2}\left[-\frac{2}{3}\left(k_{Fp}^2-\xi\right)^{3/2}\right]_0^{k_{Fp}^2} = \frac{k_{Fp}^3}{3\pi^2}. \tag{47}$$

Equation (47) naturally explains the results of Fig. 4 in $B \ll B_C(N)$. Similarly, the scalar density and the energy density are evaluated and we have the same expressions as $B = 0$:

$$\begin{aligned}
\rho_p^{(S)} &\simeq \frac{M_N^2}{\pi^2}\int_0^{k_{Fp}^2/(2M_N^2)} d\xi \int_0^{k_{Fp}(\xi)} dk\, \frac{M_p^*}{\left(k^2 + M_p^{*2} + 2\,\xi M_N^2\right)^{1/2}} \\
&= \frac{M_p^*}{\pi^2}\int_0^{k_{Fp}} d\xi\, \xi\, \ln\left(\xi + E_{Fp}\right) - \frac{M_p^*}{4\pi^2}\int_{M_p^{*2}}^{E_{Fp}^2} d\xi\, \ln\xi \\
&= \frac{1}{2\pi^2} M_p^*\left(k_{Fp}E_{Fp} - M_p^{*2}\ln\left|\frac{k_{Fp}+E_{Fp}}{M_p^*}\right|\right),
\end{aligned} \tag{48}$$

$$\begin{aligned}
\varepsilon_p &\simeq \frac{M_N^2}{\pi^2}\int_0^{k_{Fp}^2/(2M_N^2)} d\xi \int_0^{k_{Fp}(\xi)} dk \left(k^2 + M_p^{*2} + 2\,\xi M_N^2\right)^{1/2} \\
&= \frac{1}{4\pi^2}E_{Fp}\int_0^{k_{Fp}^2} d\xi \left(k_{Fp}^2 - \xi\right)^{1/2} + \frac{1}{2\pi^2}\int_0^{k_{Fp}} d\xi\, \xi\left(E_{Fp}^2 - \xi^2\right)\ln\left(\xi + E_{Fp}\right) - \frac{1}{8\pi^2}\int_{M_p^{*2}}^{E_{Fp}^2} d\xi\, \xi \ln\xi \\
&= \frac{1}{4\pi^2}k_{Fp}^3 E_{Fp} + \frac{1}{8\pi^2}M_p^{*2}\left(k_{Fp}E_{Fp} - M_p^{*2}\ln\left|\frac{k_{Fp}+E_{Fp}}{M_p^*}\right|\right).
\end{aligned} \tag{49}$$

Equations (48) and (49) imply that in $B \ll B_C(N)$ the selfconsistent equations (30)-(33) reduce to the equations of no magnetic field. Therefore, neither the renormalized mass nor the EOS depends on B. This is consistent to our results in Figs. 1-3 but contradicts the anomalous features for $B = 10^{13}G$ predicted in Ref. [12].

4. Summary

We have investigated the NS matter in magnetic field using a new RMF model, the EZM model. It is essentially different from the familiar NLW model because of the effectively density-dependent renormalized meson-nucleon coupling constants. It has stronger $NN\omega$ coupling constant being consistent to Bonn A potential and predicts a lower renormalized mass being consistent to the DBHF calculation. The EZM model is superior to the NLW and the original ZM models in the description of dense baryonic matter.

We have taken into account the anomalous magnetic moments of nucleons and the isovector-scalar mean-field according to the preceding works [11,12]. The rather strong $NN\delta$ and $NN\rho$ coupling constants are employed so as to clarify the isovector contributions. The renormalized masses and the EOSs have been calculated as functions of the total baryon density for several strengths of the magnetic field. The effect is apparent only for the stronger field than the maximum internal field of NSs expected from the scalar virial theorem. Next, we have investigated the dependencies of the renormalized masses and the particle fractions upon the magnetic field. In the weaker fields $B \ll B_C(N)$ they are constant, while the effects of Landau quantization are apparent especially in the particle fractions as the field becomes stronger.

Almost features of the magnetized NS matter in the EZM model are the same as the NLW model in Refs. [11] and [12]. However, we cannot reproduce the anomalous features for $B = 10^{13}G$ predicted in Ref. [12]. Is this due to the difference between the EZM and the NLW model? In weak magnetic fields $B \ll B_C(N)$ the Landau levels generally become almost continuous. The summation of the Landau quantum number is therefore replaced by integral of νB. Consequently, no physical quantities in the selfconsistent equations determining the renormalized masses depend on the magnetic field irrespective of the model. The anomalous features in $B = 10^{13}G$ are not likely to emerge.

Although we have taken into account nucleons only as baryons, it is well known that the hyperons [31] or more generally strange objects [32] play significant roles in the cores of compact stars. In fact, the recent works have investigated the effects of hyperons [33] and antikaon condensation [34] in magnetized NS matter. We will also investigate them within the EZM model in feature works.

References

[1] Duncan R C arXiv:astro-ph/0002442.
[2] Kouveliotou C, Duncan R C and Thompson C 2003 *Scientific American* February.
[3] Heyl J S 2005 arXiv:astro-ph/0504077.
[4] Fushiki I, Gudmudsson F H and Pethick C J 1989 *Astrophys. J.* **342** 958.
[5] Chakrabarty S, Bandyopadhyay D and Pal S 1997 *Phys. Rev. Lett.* **78** 2898 [arXiv:astro-ph/9703034].
[6] Serot B D and Walecka J D 1986 *Advances in Nuclear Physics* **16** (Plenum, New York).
[7] Alonso J D and Cabanell J M I 1985 *Astrophys. J.* **291** 208.

[8] Glendenning N K 1985 *Astrophys. J.* **293** 470.
[9] Yuan Y F and Zhang J L 1999 *Astrophys. J.* **525** 950
[10] Zimanyi J and Moszkowski S A 1990 *Phys. Rev.* C **42** 1416.
[11] Broderick A, Prakash M and Lattimer J M 2000 *Astrophys. J.* **537** 351.
[12] Wei F X, Mao G J, Ko C M, Kisslinger L S, Stöcker H and Greiner W 2006 *J. Phys.* G **32** 47 [arXiv:nucl-th/0508065].
[13] Miyazaki K 2003 Mathematical Physics Preprint Archive (mp_arc) 05-178.
[14] Miyazaki K 2003 Mathematical Physics Preprint Archive (mp_arc) 05-190.
[15] Brockmann R and Machleidt R 1990 *Phys. Rev.* C **42** 1965.
[16] Miyazaki K 2005 Mathematical Physics Preprint Archive (mp_arc) 05-261.
[17] Miyazaki K 2004 Mathematical Physics Preprint Archive (mp_arc) 05-199.
[18] Miyazaki K 2004 Mathematical Physics Preprint Archive (mp_arc) 05-206.
[19] Miyazaki K 2004 Mathematical Physics Preprint Archive (mp_arc) 05-216.
[20] Miyazaki K 2004 Mathematical Physics Preprint Archive (mp_arc) 05-224.
[21] Miyazaki K 2005 Mathematical Physics Preprint Archive (mp_arc) 05-233.
[22] Miyazaki K 2005 Mathematical Physics Preprint Archive (mp_arc) 05-243.
[23] Miyazaki K 2005 Mathematical Physics Preprint Archive (mp_arc) 05-293.
[24] Miyazaki K 2005 Mathematical Physics Preprint Archive (mp_arc) 05-325.
[25] Miyazaki K 2005 Mathematical Physics Preprint Archive (mp_arc) 05-374.
[26] Miyazaki K 2005 Mathematical Physics Preprint Archive (mp_arc) 05-427.
[27] Li B-A, Chen L-W, Ko C M, Yong G-C and Zuo W 2005 arXiv:nucl-th/0504009; Li B-A, Chen L-W, Ko C M and Steiner A W 2006 arXiv:nucl-th/0601028.
[28] Lai D and Shapiro S L 1991 *Astrophys. J.* **383** 745.
[29] Koepf W, Sharma M M and Ring P 1991 *Nucl. Phys.* A **533** 95.
[30] Sharma M M, Nagarajan M A and Ring P 1994 *Ann. of Phys.* **231** 110.
[31] Balberg S, Lichtenstadt I and Cook G B 1999 *Astrophys. J. Suppl.* **121** 515
[32] Weber F 2001 *J. Phys.* G **27** 465 [arXiv:astro-ph/0008376]; Weber F, Cuadrat A T, Ho A and Rosenfield P 2006 arXiv:astro-ph/0602047.
[33] Broderick A E, Prakash M and Lattimer J M 2002 *Phys. Lett.* B **531** 167 [arXiv:astro-ph/0111516].
[34] Dey P, Bhattacharyya A and Bandyopadhyay D 2002 *J. Phys.* G **28** 2179 [arXiv:astro-ph/0209100].

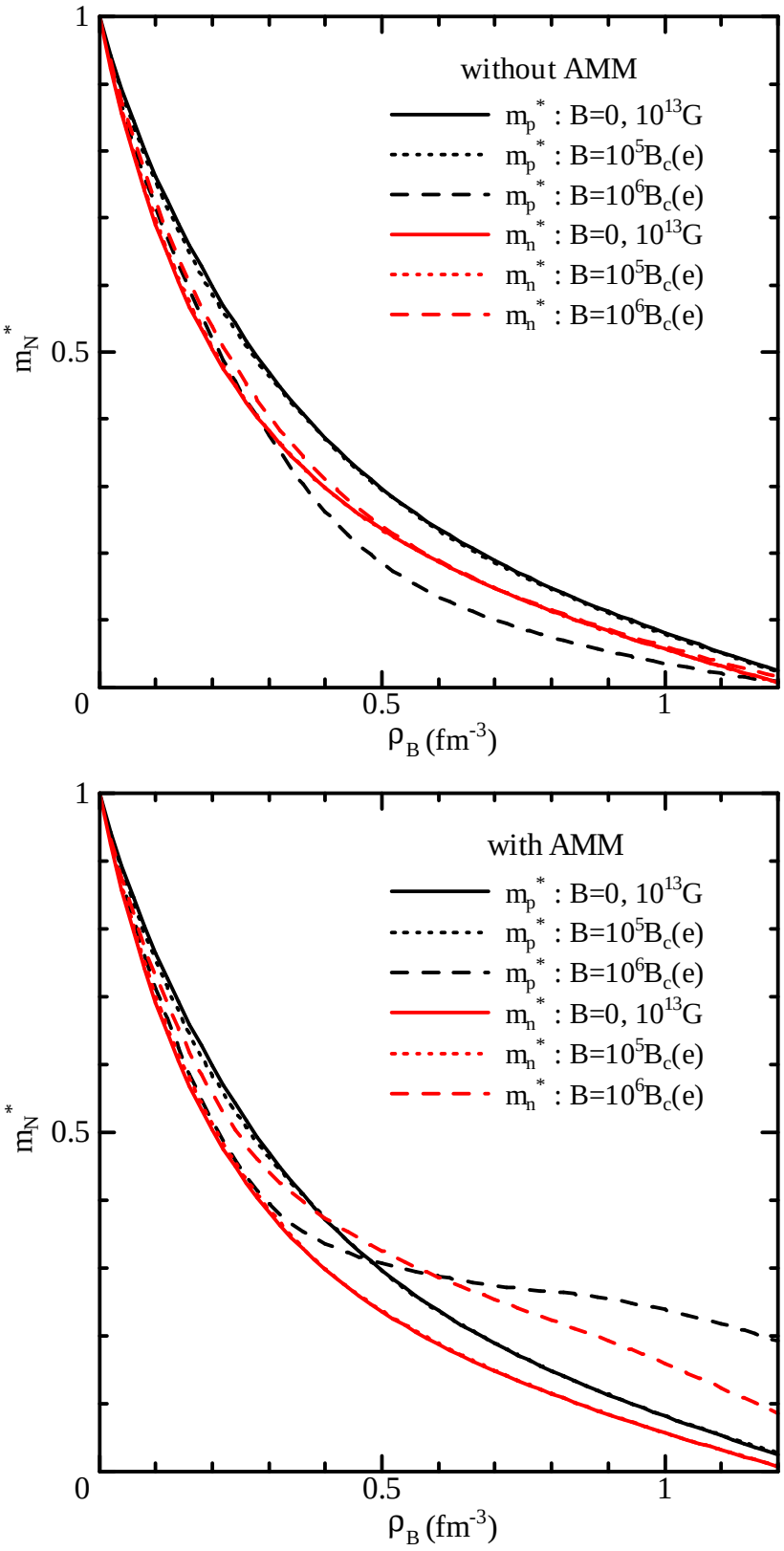

Figure 1. The renormalized masses of proton (the black curves) and neutron (the red curves) as functions of the total baryon density in the external magnetic fields $B = 0$, $10^{13}G$, $10^5 B_C(e)$ and $10^6 B_C(e)$. The upper and lower panels are without and with the anomalous magnetic moments of nucleons.

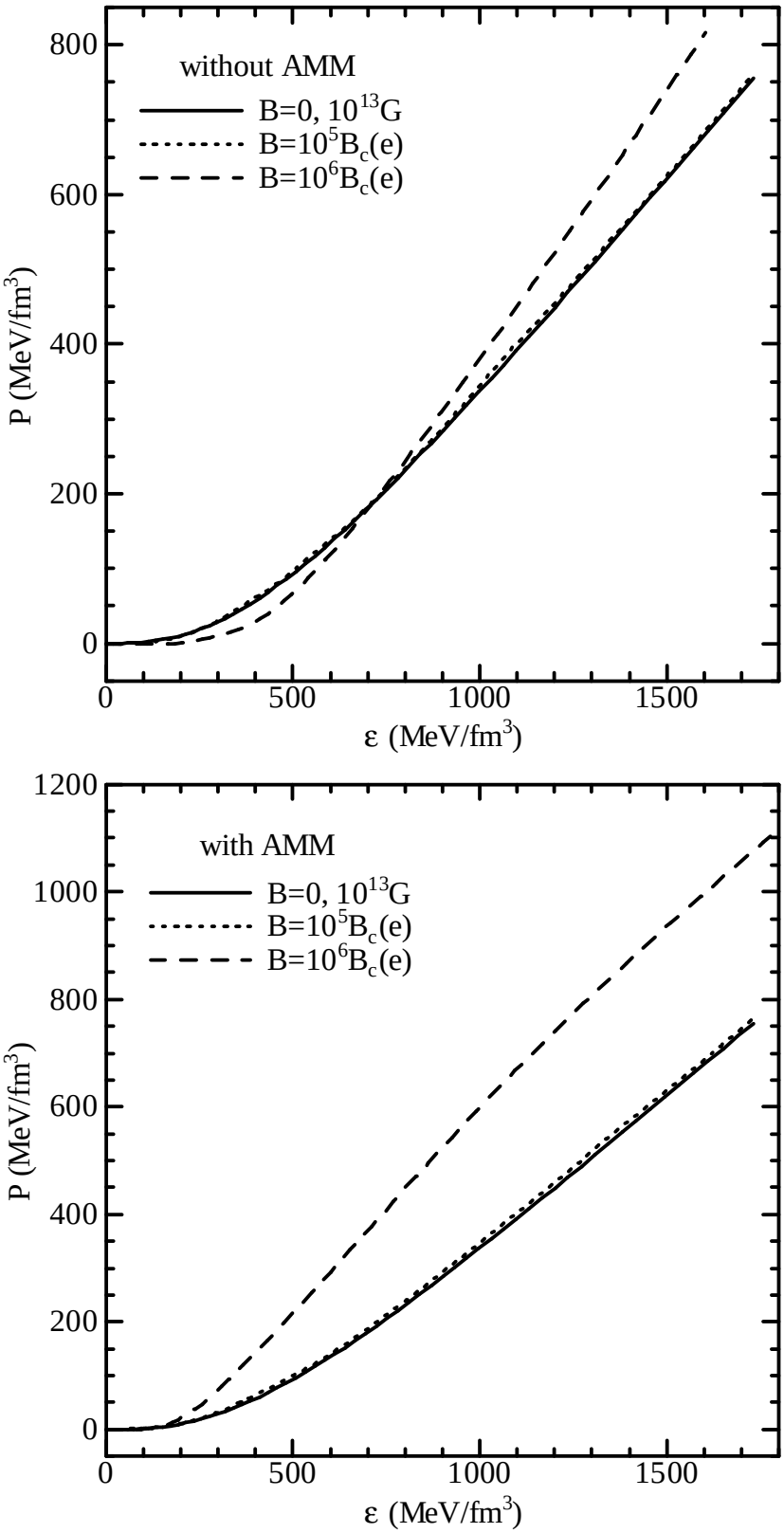

Figure 2. The EOSs of NS matter in the external magnetic fields $B = 0$, $10^{13}G$, $10^5 B_C(e)$ and $10^6 B_C(e)$. The upper and lower panels are without and with the anomalous magnetic moments of nucleons.

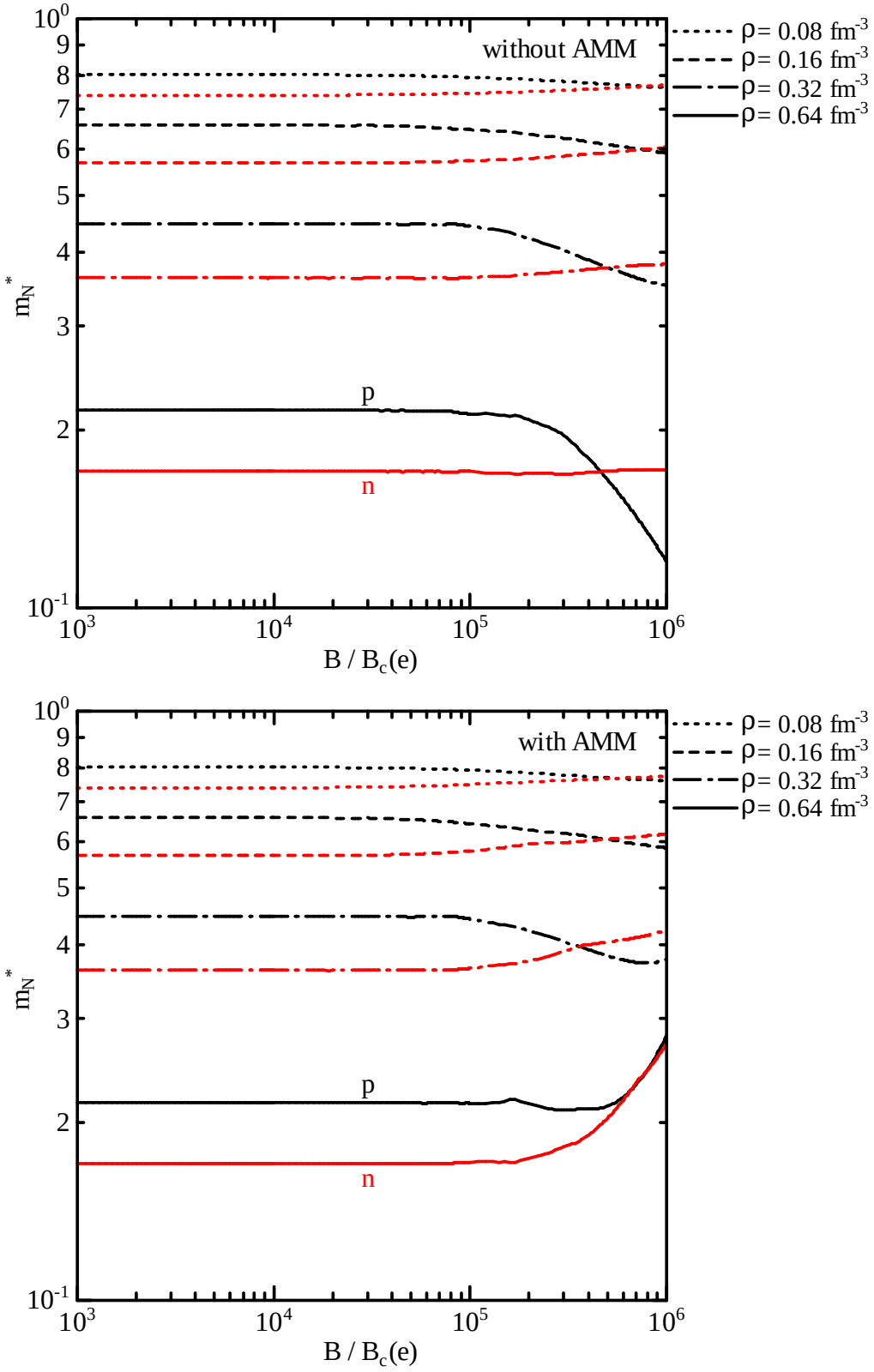

Figure 3. The renormalized masses of proton (the black curves) and neutron (the red curves) as functions of the external magnetic field. The dotted, dashed and dashed-dotted and solid curves are for $\rho_B = 0.08$, 0.16, 0.32 and 0.64 fm^{-3}, respectively. The upper and lower panels are without and with the anomalous magnetic moments of nucleons.

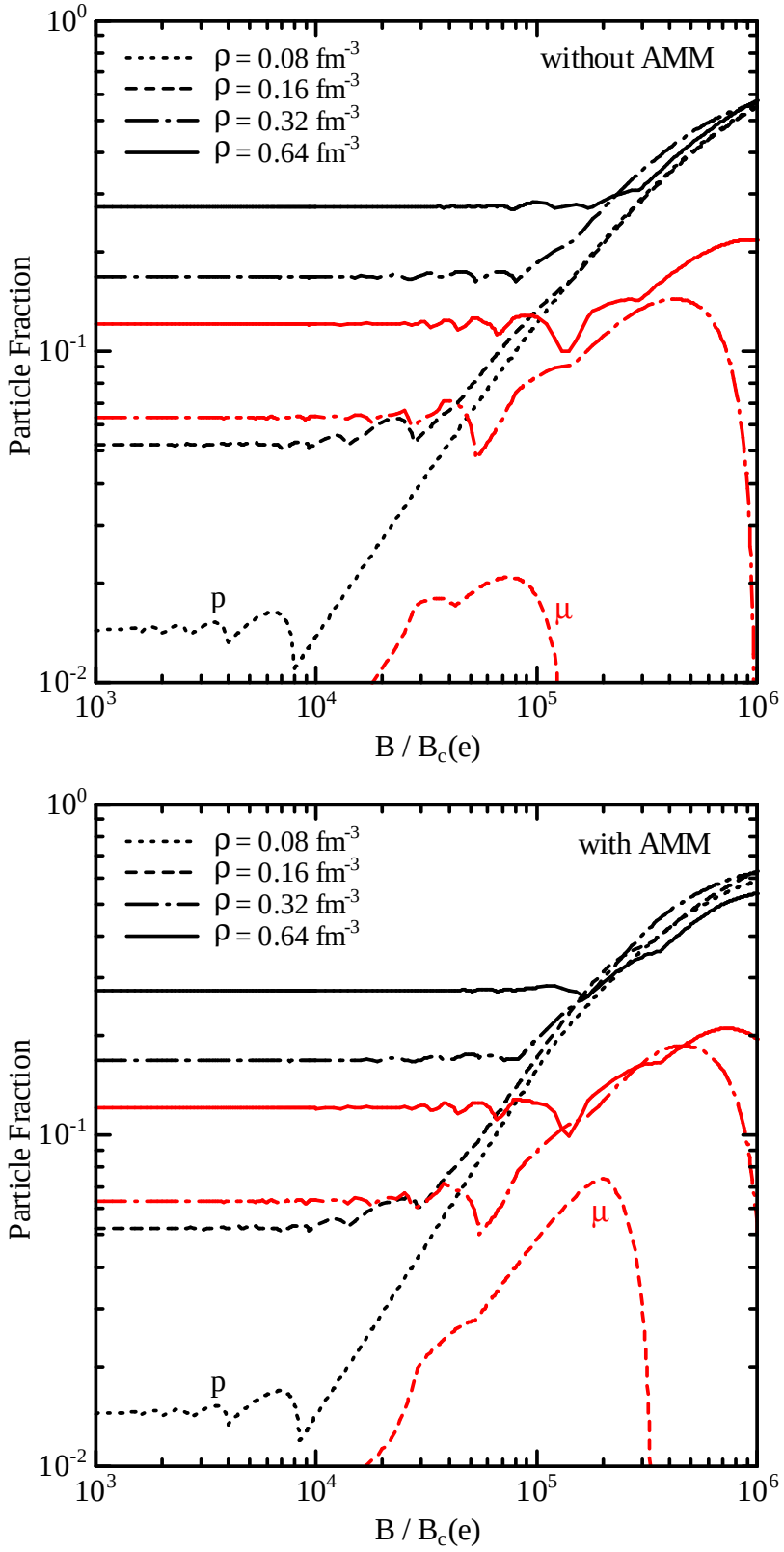

Figure 4. The fractions of proton (the black curves) and muon (the red curves) as functions of the external magnetic field. The dotted, dashed and dashed-dotted and solid curves are for $\rho_B = 0.08$, 0.16, 0.32 and $0.64\,\mathrm{fm}^{-3}$, respectively. The upper and lower panels are without and with the anomalous magnetic moments of nucleons.